JOURNAL OF SOLID STATE CHEMISTRY **126,** 15–21 (1996)
ARTICLE NO. 0303

Neutron Diffraction Study of the Nuclear and Magnetic Structure of the $CrVO_4$ Type Phosphates $TiPO_4$ and VPO_4

R. Glaum,* M. Reehuis,† N. Stüßer,† U. Kaiser,* and F. Reinauer*

*Institut f. anorg. u. analyt. Chemie, Justus-Liebig-Universität, Heinrich-Buff-Ring 58, D-35392 Gießen, Germany; and †Hahn-Meitner-Institut, Glienicker Straße 100, D-14109 Berlin, Germany

Received January 22, 1996; in revised form May 21, 1996; accepted May 30, 1996

The nuclear structures of $TiPO_4$ and VPO_4 have been refined from neutron powder data using the Rietveld technique. For both compounds, the $CrVO_4$ type nuclear structure (*Cmcm*, $Z = 4$) was confirmed at 2 K with residuals of $R_N = 0.033$ ($TiPO_4$) and $R_N = 0.022$ (VPO_4). In this structure the magnetic ions form chains running along the *c*-axis. For VPO_4, magnetic ordering with a propagation vector k = ($\frac{1}{2}$ 0 0) was found between 2 and 10.3(5) K. This magnetic structure shows antiferromagnetic intra-chain as well as inter-chain ordering. The magnetic moments are aligned parallel to the *b*-axis and reach the value ($\mu_{exp} = 0.8(1)\ \mu_B$. In the temperature range from 10.3(5) K up to the Néel point $T_N = 25.5(5)$ K an incommensurate magnetic structure with increasing k_x component of the propagation vector ($0.5 \leq k_x \leq 0.561$) was found. In contrast to the vanadium compound no magnetic ordering was detected for $TiPO_4$ down to 2 K.

INTRODUCTION

A whole series of anhydrous sulfates MSO_4 (M = Mn, Fe, Co, Ni) of divalent transition metals has been investigated by neutron diffraction (1, 2 and references therein). The crystal structures of these sulfates are closely related to those of $CrVO_4$ and the anhydrous phosphates $TiPO_4$ (5), VPO_4 (5), β-$CrPO_4$ (3), and the high-pressure modification $FePO_4$-II (4).

A general feature of this structure type with the magnetic ions occupying the (4*a*) position in space group *Cmcm* [(0 0 0), (0 0 $\frac{1}{2}$), ($\frac{1}{2}$ $\frac{1}{2}$ $\frac{1}{2}$), ($\frac{1}{2}$ $\frac{1}{2}$ 0)] is a series of chains of trans-edge-sharing octahedra similar to those observed in the rutile structure running along the crystallographic *c*-axis (Fig. 1). The magnetic structure of β-$CrPO_4$ has been determined by neutron powder investigations (3), revealing strong antiferromagnetic intra-chain coupling. Magnetic interaction between adjacent chains leads to an incommensurate magnetic superstructure with dimensions $\sim 3a_{nucl} \cdot b_{nucl} \cdot c_{nucl}$. While for β-$CrPO_4$ the magnetic moments were found to lie within the *ab*-plane (3), for the high pressure phase $FePO_4$-II (4) magnetic moments slightly tilted against the *c*-axis were proposed, leading to an overall magnetic moment per chain. Following this model, which has been derived from susceptibility and Mössbauer measurements, adjacent chains are coupled antiferromagnetically. Despite their unusual magnetic behavior (Fig. 2) no studies on the magnetic ordering in $TiPO_4$ and VPO_4 have been published so far. While for cations with half filled t_{2g} orbitals generally antiferromagnetic ordering within the chains is observed there seems to be no systematic behavior for the magnetic exchange from one chain to the next via intermediate sulfate or phosphate.

Due to uncertainties about the correct space group (5) and the possibility of the existence of a superstructure in $TiPO_4$ as a result of deviations from the high symmetrical arrangement in the oxygen positions (6) a refinement of the nuclear structure of the two orthophosphates is of additional interest.

EXPERIMENTAL

The orthophosphates $TiPO_4$ and VPO_4 were obtained as single phases according to Eqs. [1] and [2]. By chemical vapor transport suitable single crystals of VPO_4 were grown for the diffraction experiments. They were dichroic (grayish-green and brownish-red) and showed prismatic shape with the long edge parallel to the crystallographic *c*-axis and an edge-length up to 5 mm. Details on the synthesis and crystal growth have been reported earlier (5, 7).

$$4\ TiO_{2,s} + 4\ TiP_2O_{7,s} + TiP_s = 9\ TiPO_{4,s} \qquad [1]$$

$$4\ VPO_{5,s} + VP_s = 5\ VPO_{4,s} \qquad [2]$$

The neutron powder diffraction measurements were carried out on the instrument E6 at the BERII reactor of the HMI in Berlin. Attached to this instrument was a vertically and horizontally focusing graphite monochromator which used the (002) reflection (λ = 2.42 Å). The powder data of $TiPO_4$ were recorded at 2 and 298 K in the range

0022-4596/96 $18.00

$20° \leq 2\Theta \leq 80°$ (step width 0.1°) using a 20° multidetector. With the same experimental setup, neutron powder diffraction patterns for VPO_4 ($20° \leq 2\Theta \leq 60°$; step width 0.1°) were recorded at several temperatures from 2 up to 78 K.

The Rietveld refinements were carried out using the program FULLPROF (8). The neutron scattering lengths used were $b(\mathrm{Ti}) = -3.438$ fm, $b(\mathrm{V}) = -0.382$ fm, $b(\mathrm{P}) = 5.13$ fm, and $b(\mathrm{O}) = 5.805$ fm (9). The magnetic form factors of the V^{3+} ion were taken from reference (10).

A single crystal of VPO_4 ($5 \times 0.5 \times 0.5$ mm^3) was also investigated on the four-circle diffractometer E5 (BERII reactor, HMI Berlin) using a graphite monochromator, (002) reflection, with the wavelength 2.42 Å. Single crystal data were collected between 10 and 30 K using a closed cycle refrigerator. Further details of the instruments are described elsewhere (11).

RESULTS

Nuclear Structure of $TiPO_4$ and VPO_4

The Rietveld refinements for $TiPO_4$ were carried out with data sets in the range $20° \leq 2\theta \leq 70°$. A total of 15 variables were refined: overall scale factor, 5 positional parameters, 3 lattice parameters, 5 peak-shape parameters (pseudo-Voigt), and the zero-point. The isotropic thermal parameters were taken according to Ref. (5) and were held constant during the refinements even of the 2 K data due to the small data set. The results are summarized in Table 1. Figure 3 gives the observed and calculated neutron powder diffraction patterns of $TiPO_4$ at 2 and 298 K. A representation of the crystal structure of $TiPO_4$ and VPO_4 with MO_6- and PO_4-polyhedra is shown in Fig. 1.

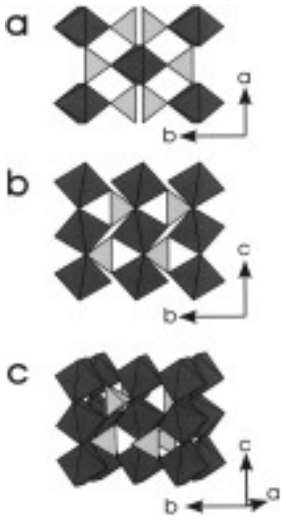

FIG. 1. Schematic representations of the crystal structure of $TiPO_4$ and VPO_4. MO_6 octahedra, dark grey; PO_4 tetrahedra, light grey. (a) projection on the *ab*-plane (along chains of edge-sharing octahedra); (b) projection on the *bc*-plane (perpendicular to the chains of edge-sharing octahedra); (c) perspective view of the crystal structure showing the linkage of octahedral chains by PO_4 tetrahedra. The structure plots were produced with the program ATOMS (15).

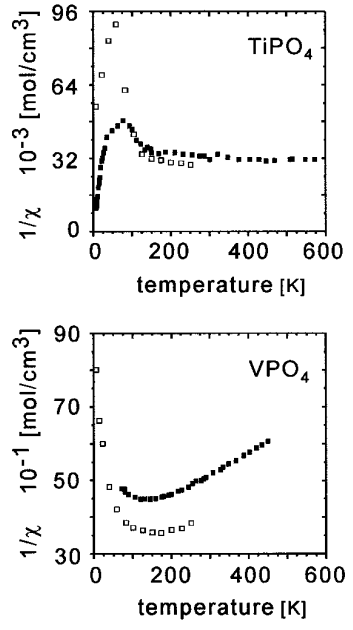

FIG. 2. Temperature dependence of the reciprocal susceptibility of $TiPO_4$ and VPO_4. (□) Magnetic behavior from 4 to 250 K measured on powders of selected crystals from chemical vapor transport experiments (5). For comparison data measured by Kinomura *et al.* (14) on powders of $TiPO_4$ and VPO_4 (■) are shown too. Differences in the susceptibility values are ascribed to the different methods of sample preparation.

For VPO_4 the nuclear structure was initially refined from data sets collected between 20° and 58° (in 2θ) on a powder sample at 26.4 and 78.0 K where no magnetic reflections are present (Fig. 4). A total of 10 variable parameters were allowed. Due to the small data sets the peak-shape parameters were held constant and the isotropic thermal parameters were treated in the same way as described for $TiPO_4$. The results of the refinements, which are in good agreement with the parameters found in X-ray single crystal investigations (5), are given in Table 1. Selected interatomic distances for $TiPO_4$ and VPO_4 are summarized in Table 2.

Magnetic Structure of VPO_4

Below the Néel temperature of VPO_4 $T_N = 25.5(5)$ K, two weak magnetic reflections were observed in the powder patterns indicating the ordering of the magnetic moments of the V^{3+} ions (Fig. 5). Neutron diffraction experiments on a single crystal of VPO_4 showed that between 2 and 10 K these reflections could be indexed as $(\frac{1}{2}\ 0\ 1)$ and $(\frac{1}{2}\ 1\ 1)$ on the basis of the primitive cell corresponding to the C-centered nuclear cell. In general these reflections can be generated by the rule $(hkl)^{\pm}_{\mathrm{mag}} = (hkl)_{\mathrm{nucl}} \pm \mathbf{k}$,

TABLE 1
Results of the Rietveld Refinements of the Neutron Powder Data of Orthorhombic Phosphates $TiPO_4$ and VPO_4

	$TiPO_4$			VPO_4			
	2 K	298 K	X-ray	2 K	26.4 K	78 K	X-ray
a [Å]	5.302(2)	5.303(2)	5.2985(5)	5.230(2)	5.239(6)	5.238(6)	5.2316(5)
b [Å]	7.899(4)	7.902(4)	7.911(1)	7.767(3)	7.787(8)	7.783(8)	7.7738(7)
c [Å]	6.310(3)	6.349(2)	6.3475(5)	6.243(2)	6.259(5)	6.261(6)	6.2847(5)
a/b	0.7988	0.8035	0.8024	0.8038	0.8038	0.8044	0.8084
y(P)	0.322(6)	0.322(4)	0.3501(2)	0.344(2)	0.356(5)	0.345(5)	0.3501(2)
x(O1)	0.239(4)	0.235(4)	0.2408(8)	0.243(2)	0.244(4)	0.241(6)	0.2408(8)
y(O1)	0.466(3)	0.459(2)	0.4630(5)	0.469(2)	0.470(3)	0.467(7)	0.4630(5)
y(O2)	0.263(3)	0.260(2)	0.2430(5)	0.2515(9)	0.252(2)	0.252(2)	0.2430(5)
z(O2)	0.047(3)	0.046(2)	0.0509(7)	0.039(3)	0.032(8)	0.039(10)	0.0509(7)
R_N (no. of F's)	0.033(11)	0.036(11)	0.062(335)	0.022(8)	0.020(8)	0.026(8)	0.049(223)

Note. The residuals R_N defined as $R_N = \Sigma(|F_o - F_c|)/\Sigma|F_o|$ (with the number of structures in parentheses) for the nuclear structure were obtained in refinements of the diffraction data between $20° \leq 2\theta \leq 70°$. The atoms Ti or V, P, O1, and O2 are in the Wyckoff positions 4*a*, 4*c*, 8*g*, and 8*f* of the space group *Cmcm*. For comparison the results from X-ray single crystal investigations (5) at 295 K are included.

where the propagation vector **k** corresponds to **k** = ($\frac{1}{2}$ 0 0). The four magnetic ions in the C-centered orthorhombic cell of the nuclear structure occupy the positions (0 0 0), (0 0 $\frac{1}{2}$), ($\frac{1}{2}$ $\frac{1}{2}$ $\frac{1}{2}$), and ($\frac{1}{2}$ $\frac{1}{2}$ 0) (Wyckoff position 4*a*). The spins on each ion can be represented by vectors $\mathbf{S}_1$, $\mathbf{S}_2$, $\mathbf{S}_3$, and $\mathbf{S}_4$, respectively. In the expected collinear case the possible antiferromagnetic structure models M_i are the following (1):

$$M_1\text{: } \mathbf{S}_1 = -\mathbf{S}_2 = -\mathbf{S}_3 = \mathbf{S}_4$$
$$M_2\text{: } \mathbf{S}_1 = \mathbf{S}_2 = -\mathbf{S}_3 = -\mathbf{S}_4$$
$$M_3\text{: } \mathbf{S}_1 = -\mathbf{S}_2 = \mathbf{S}_3 = -\mathbf{S}_4.$$

Due to the fact that the commensurate magnetic structure has a doubled *a*-axis the magnetic atoms in adjacent cells along the *a*-direction are opposite in sign according to $\mathbf{S}_i' = -\mathbf{S}_i$ (i = 1, 2, 3, 4). In this magnetic structure the models M_1 and M_3 become identical. On the other hand model M_2 is identical to a model M_4 with all spins parallel (M_4: $\mathbf{S}_1 = \mathbf{S}_2 = \mathbf{S}_3 = \mathbf{S}_4$). In our case the presence of the magnetic reflection ($\frac{1}{2}$ 0 1) and the absence of ($\frac{1}{2}$ 1 0) and ($\frac{3}{2}$ 1 0) are indicating magnetic ordering of the type M_1 (M_3).

The magnetic structure of VPO_4 was successfully refined with the moments parallel to the *b*-axis. The calculations led to a residual R_{mag} = 0.10 and a magnetic moment μ_{exp} = 0.8(1) μ_B for the powder data set measured at 2 K. Refinements of the data sets collected at 7.5 and 9.5 K do not show a significantly reduced magnetic moment of the V^{3+} ions. Due to the rather weak magnetic intensities and the resulting poor counting statistics we were not able to determine the magnetic moment with high accuracy. Data from single crystal investigations (T = 10 K) confirmed the magnetic structure. Due to better statistics a smaller residual R_{mag} = 0.029 and a magnetic moment μ_{exp} = 0.59(2) μ_B with a smaller standard deviation were obtained. A list of the observed and calculated structure factors is given in Table 3.

TABLE 2
Selected Interatomic Distances (Å) for $TiPO_4$ and VPO_4 from X-Ray Single Crystal Investigations (5) at 295 K

2x Ti–O1	1.950(2)	2x V–O1	1.928(2)
4x Ti–O2	2.119(2)	4x V–O2	2.080(2)
2x Ti–Ti^{i}	3.174(1)	2x V–V^{i}	3.140(1)
4x Ti–Ti^{ii}	4.761(1)	4x V–V^{ii}	4.679(1)

Ti and V on (0, 0, 0); Symmetry codes: (i) x, y, $\frac{1}{2} + z$; (ii) $\frac{1}{2} + x$, $\frac{1}{2} + y$, z

TABLE 3
Observed and Calculated Magnetic Structure Factors of VPO_4 (Phase I) from Single-Crystal (10 K) and Powder (2 K) Neutron Diffraction

h	k	l	F_{obs} single crystal (10 K)	F_{obs} powder (2 K)	F_{calc}
$\frac{1}{2}$	0	1	18.6	18.6	18.4
$\frac{1}{2}$	1	1	15.1	12.1	14.5
$\frac{1}{2}$	2	1	12.6	12.3	13.4
$\frac{3}{2}$	1	1	9.2	12.0	9.2

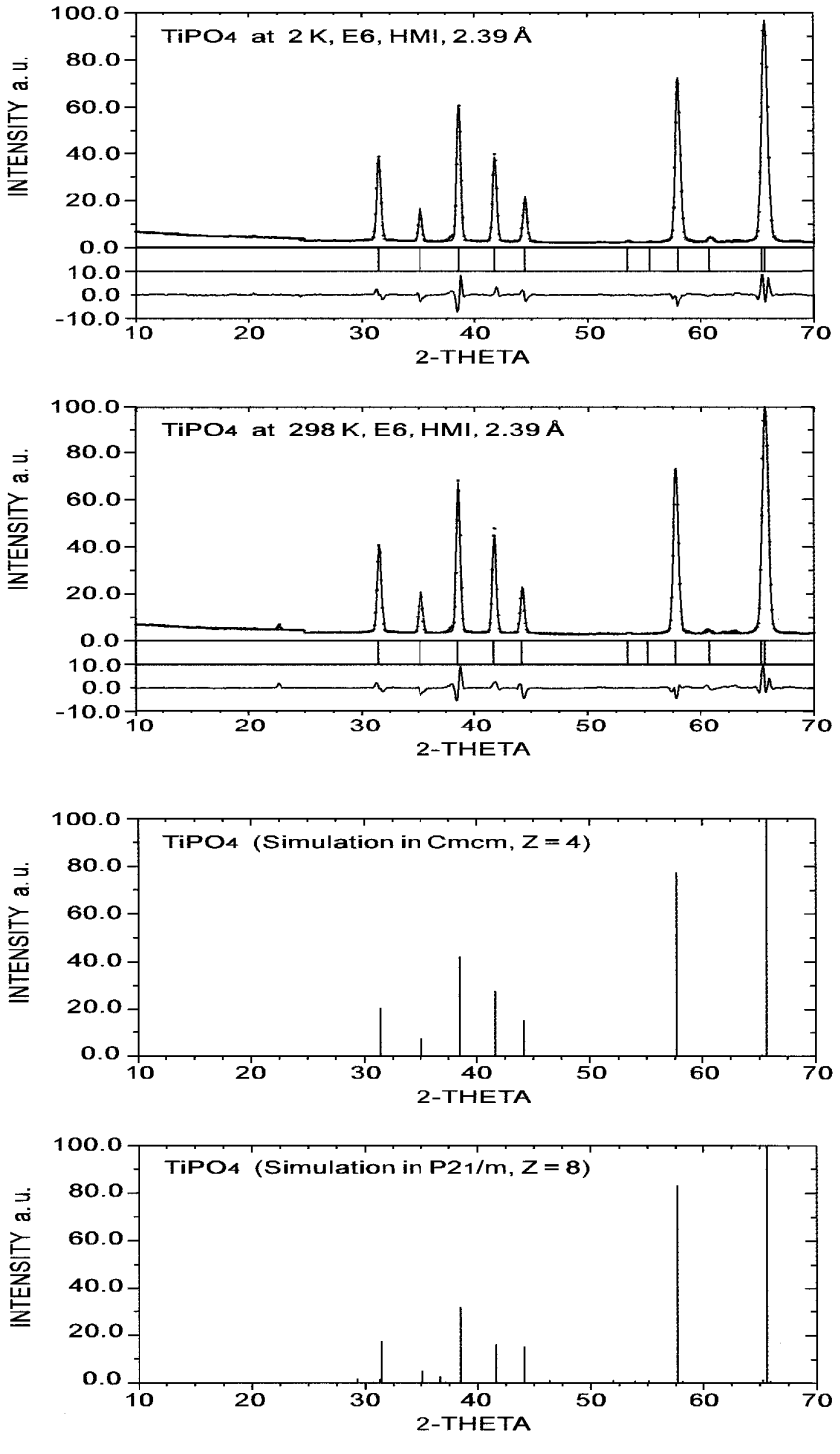

FIG. 3. Neutron powder diffraction patterns of $TiPO_4$. In the upper two diagrams collected at 2 and 300 K the observed and calculated peaks as well as the differences ($I_{obs} - I_{calc}$) are shown. In the lower part of the diagram neutron diffraction patterns calculated with the parameters obtained from the X-ray single crystal work (5) using the space group *Cmcm* ($Z = 4$) and (6) assuming $P2_1/m$ ($Z = 8$) are given.

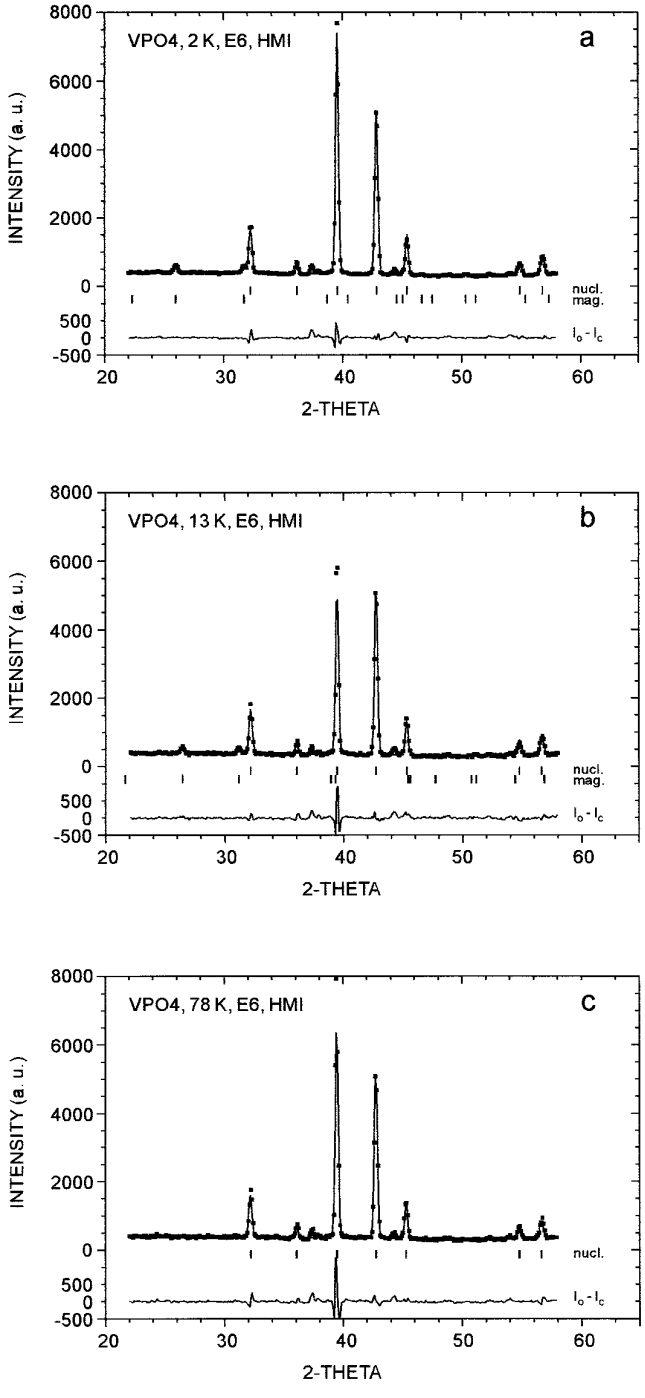

FIG. 4. Neutron powder diffraction patterns of VPO_4 at various temperatures. The observed (■) and calculated (solid line) peaks of the nuclear and magnetic structure as well as their difference are shown.

Increasing the temperature from 2 to 30 K (Fig. 6), a transition from the commensurate magnetic structure designated as phase I to an incommensurate one (phase II) is observed at $T_t = 10.3(5)$ K. Above the transition temperature the magnetic reflections $(\frac{1}{2}\,0\,1)$ and $(\frac{1}{2}\,1\,1)$ of

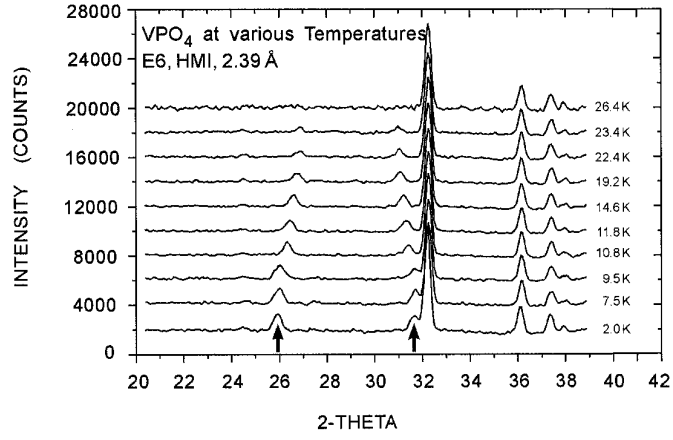

FIG. 5. Neutron powder diffraction patterns of VPO_4 in the temperature range from 2 up to 26.4 K. The positions of the magnetic reflections $(\frac{1}{2}\,0\,1)$ at $2\theta \approx 26°$ and $(\frac{1}{2}\,1\,1)$ at $2\theta \approx 32°$ are indicated.

the commensurate phase I shift apart to lower and higher 2θ angles, respectively. Investigations on a single crystal of VPO_4 revealed that only the k_x component of the propagation vector $\mathbf{k} = (k_x\,0\,0)$ shifts. The thermal variation of the value k_x was determined from powder data in the range from 2 up to 23.4 K (Fig. 7). From single crystal measurements the intensity of the reflection $(\frac{1}{2}\,0\,1)$ of phase I was found to loose approximately $\frac{1}{3}$ of its intensity (Fig. 6) with rising temperature up to 12.7 K and shifts its position to (0.52 0 1), as can be seen in Fig. 7. This magnetic reflection can be indexed in conventional notation as $(0\,0\,1)^{\pm}$ arising from a split of (0 0 1) into two overlapping satellites. The observation of only one peak requires that the reciprocal lattice vector **d** should be the same for the reflections $(0\,0\,1)^{+}$ and $(0\,0\,1)^{-}$, respectively. This is only satisfied when the propagation vector is lying within the (0 0 1) plane. From our single crystal data it was found to be $\mathbf{k} = (k_x\,0\,0)$.

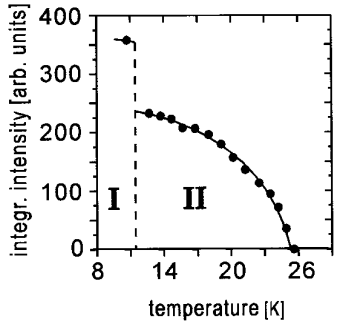

FIG. 6. Magnetic intensity of the reflection $(k_x\,0\,1)$ as function of the temperature obtained from a single crystal of VPO_4. Below 11 K the intensity is increasing spontaneously indicating the transition from the incommensurate phase II to the commensurate phase I. The solid line is only a guide for the eye.

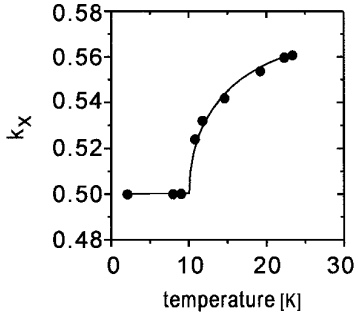

FIG. 7. Temperature dependence of the component k_x of the propagation vector $\mathbf{k} = (k_x\ 0\ 0)$ derived from a powder of VPO_4. At T_t = 10(1) K the commensurate magnetic phase I changes into the incommensurate phase II. The solid line is only a guide for the eye.

For the magnetic structure with a propagation vector $\mathbf{k} = (k_x\ 0\ 0)$ where the moments are rotating perpendicular to the *c*-axis (Fig. 8) a residual $R_{mag} = 0.13$ and a magnetic moment $\mu_{exp} = 0.7(1)\ \mu_B$ were obtained from Rietveld refinement of the data measured at 13 K. For phase II the magnetic moments in adjacent sheets are coupled antiferromagnetically like in phase I. The magnetic moment has been determined from our single crystal experiment to be $\mu_{exp} = 0.55(2)\ \mu_B$.

DISCUSSION

The neutron powder diffraction data obtained for $TiPO_4$ are in agreement with the results of the X-ray single crystal structure refinement in space group *Cmcm* ($Z = 4$). The structure refinement from neutron powder data gives no evidence for a superstructure (space group $P2_1/m$, $Z = 8$ as quoted by (6)). Simulations of the neutron powder diffraction pattern of $TiPO_4$ have been carried out with the structural data from (5) in the orthorhombic space group *Cmcm* as well as with the data from (6) in the monoclinic superstructure cell. Figure 3 compares the simulated patterns with the observed powder diagram. At least the reflection of the proposed superstructure at $2\theta = 36.71°$ should be strong enough to be observable in the neutron diffraction pattern.

The magnetic structure of VPO_4 could be determined from neutron powder and single crystal investigations. As indicated by the susceptibility measurements (Fig. 2) there is strong 1-dimensional antiferromagnetic ordering along the chains of edge-sharing octahedra even at ambient temperatures. The onset of 3-dimensional ordering is observed below 25.5 K thus suggesting much weaker inter-chain coupling. The possibility of incommensurate magnetic structures occuring under these conditions during transition from the paramagnetic to a 3-dimensionally ordered magnetic phase has been pointed out by Sólyom (12). VPO_4 and $MnWO_4$ (13) are the first examples of $CrVO_4$ type related structures, where a commensurate as well as a phase with an incommensurate magnetic structure could be observed. For all other compounds ABO_4 studied so far, only one, either commensurate or incommensurate, magnetic structure has been described (1–4).

At the present stage of the investigations only speculation about the differences in the magnetic behavior of $TiPO_4$ on one side and VPO_4 and β-$CrPO_4$ on the other is possible. In a very simple model the magnetic moments of M^{3+} (M^{3+} = Ti (d^1-system), V (d^2), Cr (d^3)) may be coupled strongly antiferromagnetically along the rutile-type chains (intra-chain coupling) by direct magnetic exchange between unpaired electrons within the t_{2g} *d*-orbital sets on the transition metal ions as well as indirectly via superexchange through bridging oxygen atoms. Inter-chain coupling should be accomplished via intermediate phosphate groups by a superexchange mechanism. In this picture the single electron on Ti^{3+} would be completely occupied by the intra-chain coupling allowing no further interactions. For VPO_4 and β-$CrPO_4$ with d^2 and d^3 configuration, respectively, on the cations superexchange would be possible through the additional *d* electrons.

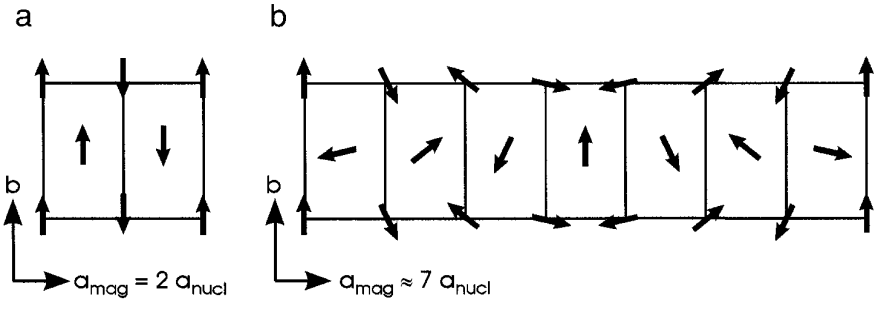

FIG. 8. (a) Commensurate magnetic structure of VPO_4 (phase I at $T < 11.7$ K; $a_{mag} = 2a_{nucl}$, $b_{mag} = b_{nucl}$, $c_{mag} = c_{nucl}$). (b) Incommensurate magnetic structure (phase II at 11.7 K $< T <$ 11.7 K; $a_{mag} \approx 7a_{nucl}$, $b_{mag} = b_{nucl}$, $c_{mag} = c_{nucl}$). In the drawings the magnetic moments of the V^{3+} ions within the (0 0 1) plane are represented by arrows. The magnetic structure of phase II is idealized taking a propagation vector $\mathbf{k}$ = (0.571 0 0), instead of $\mathbf{k}$ = (0.561 0 0), which was observed at 23.4 K, to give a periodicity of 1.75 a_{nucl}. In both magnetic phases the ordering along the *c*-axis is antiferromagnetic.

Further information about the magnetic exchange might also be obtained from studies on solid solutions of $TiPO_4$, VPO_4, and β-$CrPO_4$ with a diamagnetic phosphate like $InPO_4$. Such investigations are in progress.

ACKNOWLEDGEMENTS

This work has been supported by Deutsche Forschungsgemeinschaft.

REFERENCES

1. S. Hautecler and W. Wegner, *Phys. Stat. Sol. B* **105,** 297 (1981).
2. W. Wegner, S. Hautecler, and G. Will, *Phys. Stat. Sol. B* **105,** 491 (1981).
3. J. P. Attfield, P. D. Battle, and A. K. Cheetham, *J. Solid State Chem.* **57,** 357 (1985).
4. P. D. Battle, T. C. Gibb, G. Hu, D. C. Munro, and J. P. Attfield, *J. Solid State Chem.* **65,** 343 (1986).
5. R. Glaum and R. Gruehn, *Z. Kristallogr.* **198,** 41 (1992).
6. A. Leclaire, A. Benmoussa, M. M. Borel, A. Grandin, and B. Raveau, *Eur. J. Inorg. Solid State Chem.* **28,** 1323 (1991).
7. R. Glaum and R. Gruehn, *Z. Anorg. Allg. Chem.* **580,** 78 (1990).
8. J. Rodríguez-Carvajal, "FULLPROF: A Program for the Rietveld Refinement and Pattern Matching Analysis." Abstracts of the Satelite Meeting on Powder Diffraction of the XV Congress of the International Union of Crystallography, Toulouse, France, 1990, p. 127.
9. V. F. Sears, Atomic Energy of Canada Limited, AECL-8490, 1984.
10. P. J. Brown, *in* International Tables for Crystallography" (A. J. C. Wilson, Eds.), Vol. C, p. 391. Kluwer Academic Press, Dordrecht, 1992.
11. T. Robertson, "Neutron-Scattering-Instrumentation at the upgraded Research Reactor BER II." Berlin Neutron Scattering Center—BENSC, Berlin, 1992.
12. J. Sólyom, *Physica* **32,** 1243 (1966).
13. G. Lautenschläger, Thesis, TH Darmstadt, 1993.
14. N. Kinomura, F. Muto, and M. Koizumi, *J. Solid State Chem.* **45,** 252 (1982).
15. E. Dowty, "ATOMS for Windows. Version 3.A." Shape Software, Kingsport, TN, 1995.